Available online at www.sciencedirect.com
SCIENCE DIRECT®
Solid State Communications 130 (2004) 705–710
solid state communications
www.elsevier.com/locate/ssc

The effect of carrier density gradients on magnetotransport data measured in Hall bar geometry

L.A. Ponomarenko[a], D.T.N. de Lang[a], A. de Visser[a,*], V.A. Kulbachinskii[b], G.B. Galiev[c], H. Künzel[d], A.M.M. Pruisken[e]

[a]*Van der Waals-Zeeman Institute, University of Amsterdam, Valckenierstraat 65, 1018 XE Amsterdam, The Netherlands*
[b] *Department of Low Temperature Physics, Moscow State University, 119899 Moscow, Russia*
[c]*Institute of Ultrahigh Frequency Semiconductor Electronics, RAS, 117105 Moscow, Russia*
[d]*Fraunhofer-Institut für Nachrichtentechnik, Heinrich-Hertz-Institut, 10587 Berlin, Germany*
[e]*Institute for Theoretical Physics, University of Amsterdam, Valckenierstraat 65, 1018 XE Amsterdam, The Netherlands*

Received 23 December 2003; accepted 12 February 2004 by T.T.M. Palstra

Abstract

We have measured magnetotransport of the two-dimensional electron gas in a Hall bar geometry in the presence of small carrier density gradients. We find that the longitudinal resistances measured at both sides of the Hall bar interchange by reversing the polarity of the magnetic field. We offer a simple explanation for this effect and discuss implications for extracting conductivity flow diagrams of the integer quantum Hall effect.

PACS: 73.43.Qt; 73.43.Nq

Keywords: D. Magnetotransport; D. Quantum Hall effect

1. Introduction

The primary technique for probing the two-dimensional (2D) electron gas in semiconductor heterostructures is magnetotransport. In practice, this is realized by passing a constant current I through a Hall bar, i.e. a rectangular sample with several contact pads for sensing the longitudinal voltage V_{xx} and the transverse or Hall voltage V_{xy}. For a homogeneous sample, three voltage contacts are sufficient to determine the longitudinal and transverse resistances, $R_{xx} = V_{xx}/I$ and $R_{xy} = V_{xy}/I$. However, in the presence of macroscopic sample inhomogeneities, i.e. inhomogeneities on a scale much larger than the typical microscopic length scales of the electron gas, the resulting resistances present average values. If the length scale of the inhomogeneities is comparable to the sample size, information about the inhomogeneities can be obtained by placing additional contacts on the sample. An example of a macroscopic inhomogeneity is a spatial variation in the carrier density, such as a small gradient along the channel direction. Such gradients are common in Hall bars and arise directly from the growth process. Besides, the spatial variation might depend on the cooling procedure. The influence of macroscopic sample inhomogeneities, geometrical effects and contacts on magnetotransport data taken from Hall bars has been investigated by a number of authors. For example, von Klitzing and Ebert [1] investigated a Hall bar with a fairly large carrier density variation ($\sim 10\%$). They reported differences in the longitudinal resistances measured on both sides of the Hall bar, as well as a strong dependence of the amplitude of the Shubnikov–de Haas oscillations on the magnetic field polarity. Geometrical effects of Hall bars, such as the influence of the channel width, the position of contacts, etc. have been investigated in detail by Haug [2], who observed, for instance, an asymmetric Shubnikov–de Haas effect on a long Hall bar without noticeable carrier density gradients. This effect persisted when the direction of

* Corresponding author. Tel.: +31-20-525-5732; fax: +31-20-525-5788.
E-mail addresses: devisser@science.uva.nl (A. de Visser), leonidp@science.uva.nl (L.A. Ponomarenko).

0038-1098/$ - see front matter © 2004 Elsevier Ltd. All rights reserved.
doi:10.1016/j.ssc.2004.02.021

the magnetic field was reversed and was attributed to the proximity of the voltage and current contacts on the Hall bar. The influence of the contact geometry and size has been studied experimentally by e.g. Woltjer et al. [3] These authors explained a number of unusual observations in terms of a local resistivity tensor.

In the course of a low-temperature magnetotransport study of the quantum Hall effect, we noted an interesting phenomenon in the R_{xx} data: upon reversing the polarity of the magnetic field the longitudinal resistances measured on top and bottom sides of the Hall bar, R_{xx}^{t} and R_{xx}^{b}, interchange. Different values of R_{xx}^{t} and R_{xx}^{b}, are quite common for Hall bars and are generally attributed to sample inhomogeneities ($R_{xx}^{t} = R_{xx}^{b}$ for a perfect Hall bar). However, the interchange of R_{xx}^{t} and R_{xx}^{b} upon field reversal cannot be accidental and requires a non-trivial explanation. Moreover, the interchange of R_{xx}^{t} and R_{xx}^{b} was found to be a generic feature of the samples investigated.

In this paper, we present magnetotransport data obtained from various quantum wells. All samples showed the interchange of R_{xx}^{t} and R_{xx}^{b} upon field reversal. We offer a simple explanation for this phenomenon, namely a small carrier gradient along the channel direction of the Hall bar. For the sake of clarity we stress that we do not report here on the well-known reverse-field reciprocity for conducting specimens in a magnetic field [4,5], which says that upon reversing the polarity of the magnetic field, the same resistance is obtained when the voltage and current contacts are interchanged.

The results presented here are important for the study of conductivity flow diagrams of the quantum Hall effect. They show that complications may arise when critical conductivities are extracted in the standard fashion from experimentally obtained resistivities on the plateau–plateau transitions.

2. Experimental

Magnetotransport experiments have been performed on different semiconductor structures: high-mobility ($\mu \sim 300,000\ \mathrm{cm^2/V\ s}$) GaAs/AlGaAs quantum wells and low-mobility ($\mu \sim 20,000\ \mathrm{cm^2/V\ s}$) GaInAs/AlInAs quantum wells. The electron densities for all our samples were fairly low ($n_e = 1.8–6.1 \times 10^{11}\ \mathrm{cm^{-2}}$), such that all samples showed distinct quantum Hall features within our available magnetic field range ($B \leq 8$ T). In some cases the electron density was increased by illumination with a LED at $T = 4.2$ K. Samples were selected such that no carrier relaxation occurred during the measurements. Throughout this paper we label the voltage contacts on the Hall bar as sketched in Fig. 1, where V_{xx}^{t} refers to contacts 3–4 and V_{xx}^{b} to 5–6. The experiments were performed in an adsorption-pump operated ^{3}He cryostat, equipped with a superconducting magnet ($B_{max} = 8$ T). The longitudinal and transverse resistance were measured simultaneously, using standard lock-in techniques at a frequency of 13 Hz. The excitation current ranged from 5 to 50 nA. The data presented here were all taken at $T = 0.4$ K.

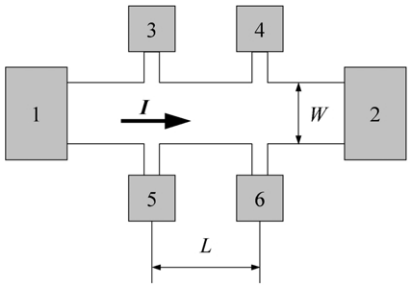

Fig. 1. Schematic picture of a Hall bar. L denotes the distance between the longitudinal voltage contacts and W the channel width.

3. Magnetotransport results: antisymmetry in R_{xx}

In Fig. 2 we show the Hall resistance between 3 and 8 T, before illumination, of the GaAs/AlGaAs quantum well (sample #659, $L \times W = 1260 \times 1000\ \mu\mathrm{m}^2$) measured at the left (3–5) and right (4–6) contact pairs across the Hall bar. The left and right Hall resistance traces, $R_{xy}^{l} = R_{xy}^{35} = (V_3 - V_5)/I$ and $R_{xy}^{r} = R_{xy}^{46} = (V_4 - V_6)/I$, were measured during the same field sweep. Upon reversing the magnetic field, R_{xy}^{l} and R_{xy}^{r} stay identical, except for the change in sign as it should: $R_{xy}^{l,r}(B) = -R_{xy}^{l,r}(-B)$. This implies that the contribution of R_{xx} to the Hall resistance is absent and that misalignment of Hall voltage contacts is negligible. The plateau–plateau (PP) transitions measured at contacts 4–6 are shifted along the field axis with respect to those at contacts 3–5. This is due to different local filling factors, $\nu(x, y) = hen_e(x, y)/B$. Assuming a constant magnetic field

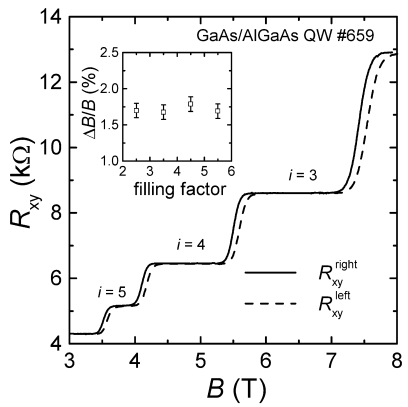

Fig. 2. Hall resistance as a function of magnetic field for the GaAs/AlGaAs quantum well (#659—no illumination) near plateaux $i = 2–6$ at $T = 0.4$ K. The solid and dashed lines show data taken at the right and left Hall contact pairs. The insert shows the relative difference between the plateau–plateau transition fields $\Delta B/B$ as a function of the filling fraction.

over the sample, the spatial distribution of filling factors matches that of the electron density n_e. Hence, the filling factor between contacts 3 and 5 is always larger than the one between 4 and 6. However, their ratio is field independent and equal to the ratio of local densities. This is corroborated by the insert in Fig. 2, where we have traced the experimental values of the shift $\Delta B/B$, measured halfway the PP transitions, versus filling factor $2 < \nu < 6$. We extract a carrier density difference $\Delta n_e/n_e = \Delta B/B = 0.017$.

Next, we present in Fig. 3 the longitudinal resistances $R^t_{xx} = R^{34}_{xx} = (V_3 - V_4)/I$ and $R^b_{xx} = R^{56}_{xx} = (V_5 - V_6)/I$ of sample #659, measured at top and bottom sides of the Hall bar. Data are taken for field up ($B\uparrow$) and down ($B\downarrow$) directions ($|B| \leq 8$ T). The data show the familiar Shubnikov-de Haas oscillations at low fields and the resistance peaks associated with the PP transitions in the quantum Hall regime at higher fields. For a homogeneous Hall bar we expect $R^b_{xx} = R^t_{xx}$, which is clearly not the case here. Instead, we find a large difference in the peak values R^b_{xx} and R^t_{xx}, which amounts up to 50% for the $i = 3 \rightarrow 2$ transition. Moreover, a close inspection of Fig. 3 shows that R^t_{xx} for $B\uparrow$ equals R^b_{xx} for $B\downarrow$ and vice versa to within 1%. We conclude that the longitudinal resistance when measured on both sides of the Hall bar shows a remarkable 'antisymmetry':

$$R^t_{xx}(B) = R^b_{xx}(-B). \quad (1)$$

After illumination, the GaAs/AlGaAs quantum well becomes more homogeneous as expected. Magnetotransport data near the $i = 6 \rightarrow 5$ PP transition are shown in Fig. 4. The carrier density increases from 4.7 to 6.1×10^{11} cm^{-2}, while the carrier difference decreases to $\Delta n_e/n_e = 0.0025$. The longitudinal resistance still remains antisymmetric, but the effect is now much smaller and amounts to only 20% for the $i = 6 \rightarrow 5$ PP transition.

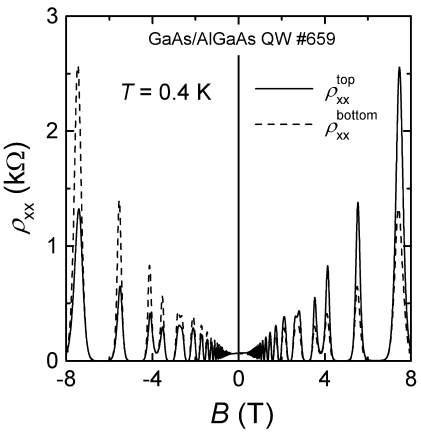

Fig. 3. Longitudinal resistivity as a function of magnetic field ($B\uparrow$ and $B\downarrow$) for a GaAs/AlGaAs quantum well (#659—no illumination). The solid and dashed lines show data taken at contact pairs located at the top and bottom side of the Hall bar. Upon reversing the magnetic field we observe an antisymmetry in the longitudinal resistivity components $\rho^t_{xx}(-B) = \rho^b_{xx}(B)$.

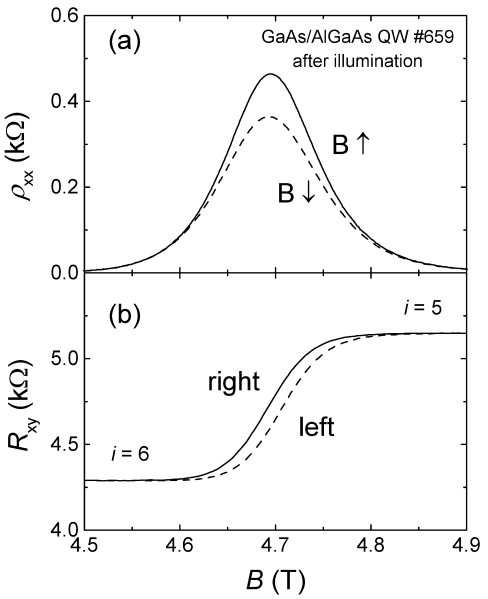

Fig. 4. Longitudinal resistivity and Hall resistance of the GaAs/AlGaAs quantum well (#659) after illumination ($T = 0.4$ K). Data are shown for the $i = 6 \rightarrow 5$ plateau–plateau transition. Upper panel: ρ_{xx} data measured at the same contact pair for two directions of B as indicated. Lower panel: R_{xy} data measured at right and left Hall contact pairs as indicated.

Magnetotransport data for the GaInAs/AlInAs quantum well ($L \times W = 387 \times 75$ μm^2) are shown in Figs. 5 and 6. Again, we show the data before illumination ($n_e = 1.8 \times 10^{11}$ cm^{-2}). From Fig. 5 we extract $\Delta n_e/n_e = 0.014$. The antisymmetry effect (Fig. 6) is not as pronounced as for the GaAs/AlGaAs quantum well, but nevertheless significant. After illumination ($n_e = 3.6 \times 10^{11}$ cm^{-2}) $\Delta n_e/n_e = 0.006$ and the antisymmetry effect is reduced. Magnetotransport

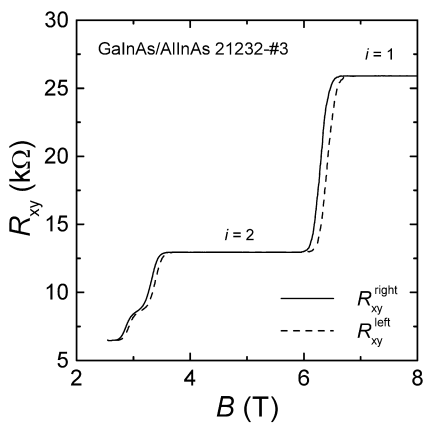

Fig. 5. Hall resistance as a function of magnetic field for the GaInAs/AlInAs quantum well (21232-#3—no illumination) near plateaux $i = 1$–3 at $T = 0.4$ K. The solid and dashed lines show data taken at the right and left Hall contact pairs.

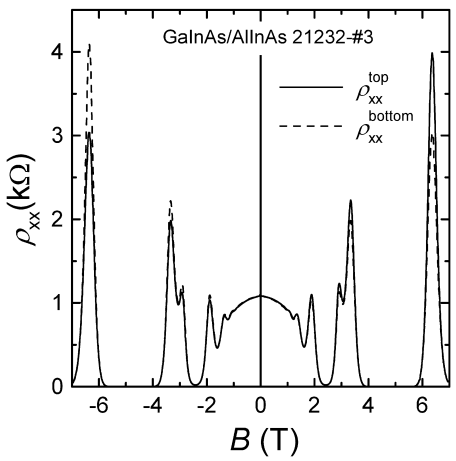

Fig. 6. Longitudinal resistivity as a function of magnetic field ($B\uparrow$ and $B\downarrow$) for the GaInAs/AlInAs quantum well (21232-#3—no illumination) at $T = 0.4$ K. The solid and dashed lines show data taken at contact pairs at the top and bottom side of the Hall bar.

measurements on a second Hall bar, prepared from the same wafer, with $n_e = 2.2\times10^{11}$ cm^{-2} show a comparable $\Delta n_e/n_e \sim 0.018$ and the corresponding antisymmetry effect.

4. The effect of a carrier density gradient

In the following we show that the observed asymmetry effect can be accounted for by a small carrier density gradient in the sample. Let us assume that the carrier density gradient points from the left current contact to the right one. In this case, R^{l}_{xy} and R^{r}_{xy} are slightly different. We define

$$\Delta R_{xy} = R^{l}_{xy} - R^{r}_{xy}, \tag{2}$$

and for the difference in the longitudinal resistances measured at both sides of the Hall bar

$$\Delta R_{xx} = R^{t}_{xx} - R^{b}_{xx}. \tag{3}$$

For a perfect Hall bar $\Delta R_{xy} = 0$ and $\Delta R_{xx} = 0$. Since

$$\Delta R_{xy} = ((V_3 - V_5) - (V_4 - V_6))/I$$
$$= ((V_3 - V_4) - (V_5 - V_6))/I = \Delta R_{xx}, \tag{4}$$

a finite ΔR_{xy} immediately implies that there is a difference between the longitudinal resistances measured at the top and bottom side of the Hall bar, $\Delta R_{xx} \neq 0$. Because the Hall voltage is an odd function of the magnetic field, reversing the polarity changes the sign of both ΔR_{xy} and ΔR_{xx}:

$$\Delta R_{xy}(-B) = -\Delta R_{xy}(B), \tag{5}$$

and

$$\Delta R_{xx}(-B) = -\Delta R_{xx}(B). \tag{6}$$

Thus ΔR_{xx} is an antisymmetric function, which holds under the conditions of Eq. (1). Eq. (4) may be directly verified by comparing the differences $\Delta R_{xx}(B)$ and $\Delta R_{xy}(B)$ calculated from the measured data (compare for instance $\Delta R_{xx} = (L/W)\Delta\rho_{xx}$ in Fig. 4(a) with ΔR_{xy} in Fig. 4(b)).

5. Plateau–plateau transitions

The effect of a carrier density gradient on the magnetotransport data as described here is in fact generally applicable to any 2D and 3D system, as follows from Eq. (4). However, the effect can be dramatically large for 2D quantum Hall samples, because of the steep slope of $R_{xy}(B)$ at the plateau–plateau (PP) transitions. Consequently, our findings yield important constraints on the construction of the conductivity flow diagrams of the PP transitions [6]. In the following paragraphs, a formal treatment of magnetotransport at the PP transition in the presence of a small carrier density gradient is presented.

We start from the usual equations for the Hall bar geometry, which tell us that a uniform current density j_x results from an applied electric field E_x along the channel direction (x):

$$E_x = \rho_0 j_x, \qquad E_y = \rho_H j_x. \tag{7}$$

Here $j_y = 0$ and ρ_0 and ρ_H are the longitudinal and Hall resistivity for a perfectly homogeneous sample. In a simple model for sample inhomogeneities we assume that the critical field B^* or filling fraction ν^* for the PP transition varies linearly in x due to a gradient in the carrier density. At the PP transition the Hall resistivity slopes from one Hall plateau to the other, while the longitudinal resistivity forms a peak, so that $|\partial\rho_H/\partial B| \gg |\partial\rho_0/\partial B|$. As such, an x-dependence of the local filling factor $\nu(x)$ therefore mainly affects the electric field component E_y:

$$E_x = \rho_0 j_x, \qquad E_y = (\rho_H + \alpha x) j_x, \qquad \alpha = \frac{\partial\rho_H}{\partial\nu}\frac{\partial\nu}{\partial x}. \tag{8}$$

This result, however, violates an important condition for having a stationary state, i.e. the electric field must be rotation free $\nabla\times\mathbf{E} = 0$. To satisfy this condition we proceed by inserting a y-dependent current density $j_x \rightarrow j_x(1+\beta y)$, where $\beta = \alpha/\rho_0$. Working to linear order in the coordinates x and y we can write

$$E_x = (\rho_0 + \rho_0\beta y) j_x, \qquad E_y = (\rho_H + \alpha x + \rho_H\beta y) j_x. \tag{9}$$

Hence

$$E_x = (\rho_0 + \alpha y) j_x, \qquad E_y = (\rho_H + \alpha x + \alpha\frac{\rho_H}{\rho_0} y) j_x, \tag{10}$$

are the appropriate equations for the PP transition. Notice that the stationary state condition $\nabla\times\mathbf{E} = 0$ and charge conservation $\nabla\cdot\mathbf{j} = 0$ are satisfied.

The longitudinal resistance at the top and bottom and the Hall resistance at the left and right contacts of the Hall bar

are given by

$$R^{t}_{xx} = V^{t}_{xx}/I_x = \frac{L}{W}\left(\rho_0 + \alpha\frac{W}{2}\right), \tag{11}$$

$$R^{b}_{xx} = V^{b}_{xx}/I_x = \frac{L}{W}\left(\rho_0 - \alpha\frac{W}{2}\right), \tag{12}$$

$$R^{l}_{xy} = V^{l}_{xy}/I_x = \left(\rho_H - \alpha\frac{L}{2}\right), \tag{13}$$

$$R^{r}_{xy} = V^{r}_{xy}/I_x = \left(\rho_H + \alpha\frac{L}{2}\right), \tag{14}$$

where we take zero coordinates (x, y) at the center of the Hall bar. When $B \rightarrow -B$, ρ_H and α change sign, but ρ_0 remains unchanged. The results therefore explain the observed asymmetry at the PP transition, $R^{b}_{xx}(B^*) = R^{t}_{xx}(-B^*)$. Notice that with this specific form of α, Eqs. (13) and (14) can be regarded as a Taylor expansion of a local Hall resistance ρ_H at values $x = \pm L/2$.

6. Discussion

Eqs. (11)–(14) show that the probed Hall resistance R_{xy} is a local resistance, and that the longitudinal resistance R_{xx} is not identical under field reversal. This gives rise to complications in extracting the conductivity components $\sigma_{xx} = \rho_{xx}/(\rho^2_{xx} + \rho^2_{xy})$ and $\sigma_{xy} = \rho_{xy}/(\rho^2_{xx} + \rho^2_{xy})$ of the PP transitions. As an example we show in Fig. 7 the σ_{xx}, σ_{xy} conductance plane with data for the $i = 4 \rightarrow 3$ and $3 \rightarrow 2$ PP transitions of the GaAs/AlGaAs quantum well (before illumination). By choosing different combinations of R^{t}_{xx} or R^{b}_{xx} and R^{l}_{xy} or R^{r}_{xy} we obtain four different σ_{xx}, σ_{xy} curves for one field direction (for the reverse field direction identical curves are obtained, but the R_{xx}, R_{xy} labelling is different). Clearly, all curves show strong deviations from the 'ideal' semicircle relation [6,7] $\sigma^2_{xx} + (\sigma_{xy} - n\sigma^*)^2 = (\sigma^*)^2$ with $\sigma^* = e^2/2h$ and $n = 7$ and 5 for the $i = 4 \rightarrow 3$ and $3 \rightarrow 2$ PP transitions, respectively. After illumination, the density increases and the sample becomes more homogeneous as can be concluded from Fig. 8(a), where we show σ_{xx}, σ_{xy} for the $i = 6 \rightarrow 5$ PP transition. Since we understand the origin of the antisymmetry upon field reversal, we can calculate an improved σ_{xx}, σ_{xy} diagram by using corrected R_{xx} and R_{xy} data, where $R_{xx} = (R^{t}_{xx} + R^{b}_{xx})/2$ and $R_{xy}(B)$ is obtained by shifting $R^{r}_{xy}(B)$ over a value of $+\Delta B/2$ along the magnetic field axis (or R^{l}_{xy} over $-\Delta B/2$). Using the corrected values for the resistances, we construct the σ_{xx}, σ_{xy} diagram shown in Fig. 8(b), which follows quite close the semicircle relation with $n = 11$.

Temperature driven σ_{xx}, σ_{xy} flow diagrams are an important experimental test of the two-parameter renormalization group theory of the quantum Hall effect [6,8]. In the scaling theory of the quantum Hall effect [6] the critical resistivity $\rho_0(B^*)$ (or critical conductivity $\sigma_0(B^*) = \sigma^*$) at the PP transition is a constant when $T \rightarrow 0$. The presence of a carrier density gradient, therefore, brings about a second complication in analyzing magnetotransport data, as the parameter α varies with temperature through $\partial\rho_H/\partial\nu$, namely a strong temperature variation of $R^{t,b}_{xx}(B^*)$. The temperature dependence of the measured critical resistance

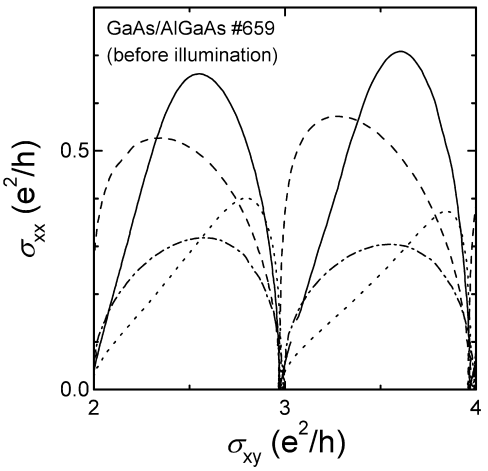

Fig. 7. The longitudinal conductance σ_{xx} as a function of the Hall conductance σ_{xy} for the $i = 4 \rightarrow 3$ and $3 \rightarrow 2$ PP transitions of the GaAs/AlGaAs quantum well before illumination ($T = 0.4$ K). The four different lines are obtained by using all possible combinations of ρ_{xx} and R_{xy}.

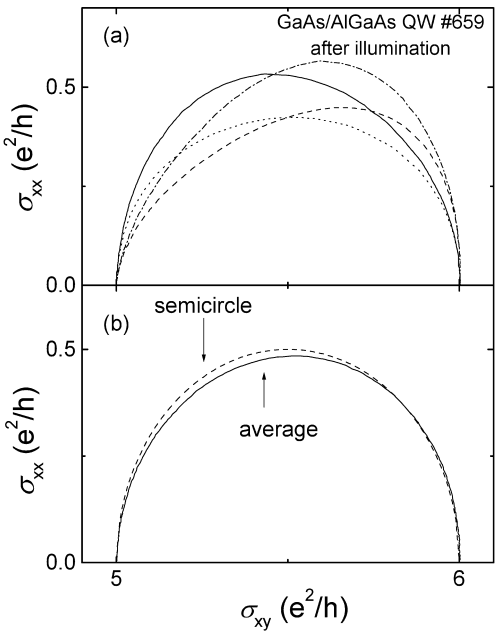

Fig. 8. (a) The longitudinal conductance σ_{xx} as a function of the Hall conductance σ_{xy} for the $i = 5 \rightarrow 6$ PP transition of the GaAs/AlGaAs quantum well after illumination ($T = 0.4$ K). The four different lines are obtained by using all possible combinations of ρ_{xx} and R_{xy}. (b) The solid line represents the σ_{xx}, σ_{xy} data after averaging. The dashed line shows the "ideal" semicircle relation.

at the PP transition, Eqs. (11)–(12), can be written as

$$R_{xx}^{t,b}(B^*,T) \propto (1 \pm \text{const}\ \alpha(T)). \quad (15)$$

Notice that when $B \rightarrow -B$ the amplitudes change according to $R_{xx}^{t}(B^*,T) = R_{xx}^{b}(-B^*,T)$. Corresponding changes in amplitude occur in the conductivities $\sigma_{xx}(B^*)$ evaluated from R_{xx}^{t} or R_{xx}^{b}. This feature of density gradients has been noticed in InGaAs/InP heterostuctures [9]. The strong temperature variation of $\sigma_{xx}(B^*)$ is removed at low temperatures when averaging the data sets obtained for both directions of the magnetic field. Thus, reversing the magnetic field is of paramount importance in determining the proper temperature variation of the conductivity peak height $\sigma_{xx}(B^*)$. The temperature variation of $\sigma_{xx}(B^*)$, reported in the literature at several places [10,11], might thus well be the result of not averaging the magnetotransport data over up and down magnetic field directions. This suggests that the occurrence of a 'non-universal' critical conductivity can be explained without the need to evoke percolation models with macroscopic fluctuations of the local filling factor [12].

The analysis of the PP transition has been made for Hall bars with a constant density gradient along the channel direction. In a real sample, the situation may be more complex (gradients in x–y directions, non-linear density variations). In addition, intrinsic sample inhomogeneities can also lead to Hall potential contact misalignment, which in general gives rise to a contribution from R_{xx} to the R_{xy} data. In Ref. [13] a novel analytical procedure was presented to disentangle the universal quantum critical aspects of the magnetotransport data and sample dependent aspects, such as density gradients and contact misalignment. The methodology is based on decomposing the measured ρ_{ij} in symmetric and antisymmetric parts, as made here for the most simple case. So far, the analysis has been applied successfully to the plateau–insulator (PI) phase transition measured for an InGaAs/InP heterostructure [9,13]. At the PI transition, $R_{xy} \sim h/e^2$ remains quantized which facilitates the analysis. At the PP transition the situation is much more complex, as both ρ_{xx} and ρ_{xy} are a function of T and B.

7. Conclusions

The effect of macroscopic sample inhomogeneities on magnetotransport data of the 2D electron gas in the Hall bar geometry has been investigated. We find a remarkable antisymmetry in the longitudinal resistances R_{xx}^{t} and R_{xx}^{b} measured on both sides of the Hall bar upon reversing the magnetic field: $R_{xx}^{t}(B) = R_{xx}^{b}(-B)$. The antisymmetry in R_{xx} is explained by a small carrier gradient along the channel direction of the Hall bar. The presence of a carrier density gradient complicates the study of quantum criticality of the plateau–plateau transitions in the quantum Hall effect. We evaluate expressions for the resistances at the plateau–plateau transitions and demonstrate complications that arise in extracting σ_{xx}, σ_{xy} flow diagrams.

Acknowledgements

This work was supported by FOM (Dutch Foundation for Fundamental Research of Matter). V.A.K. and G.B.G were supported by research grant RFBR 00-02-17493. The authors would like to thank Peter Nouwens from the Technical University Eindhoven for the preparation of Hall bars and Paul Koenraad for valuable discussions.

References

[1] K. von Klitzing, G. Ebert, in: G. Bauer, F. Kuchar, H. Heinrich (Eds.), Two-dimentional Systems, Heterostructures and Superlattices, Springer, Berlin, 1984, p. 243.
[2] R.J. Haug, Semicond. Sci. Technol. 8 (1993) 131.
[3] R. Woltjer, M.J.M. de Blank, J.J. Harris, C.T. Foxon, J.P. André, Phys. Rev. B 38 (1988) 13297.
[4] H.H. Sample, W.J. Bruno, S.B. Sample, E.K. Kichel, J. Appl. Phys. 61 (1987) 1079.
[5] M. Büttiker, Phys. Rev. Lett. 57 (1986) 1761.
[6] A.M.M. Pruisken, Phys. Rev. Lett. 61 (1988) 1297.
[7] A.M. Dykhne, I.M. Ruzin, Phys. Rev. B 50 (1994) 2369.
[8] H.P. Wei, D.C. Tsui, A.M.M. Pruisken, Phys. Rev. B 33 (1985) 1488.
[9] D.T.N. de Lang, L.A. Ponomarenko, A. de Visser, A.M.M. Pruisken, to be published.
[10] H.P. Wei, S.Y. Lin, D.C. Tsui, A.M.M. Pruisken, Phys. Rev. B 45 (1992) 3926.
[11] L.P. Rokhinson, B. Su, V.J. Goldman, Solid State Commun. 96 (1995) 309.
[12] I.M. Ruzin, N.R. Cooper, B.I. Halperin, Phys. Rev. B 53 (1996) 1558.
[13] A.M.M. Pruisken, D.T.N. de Lang, L.A. Ponomarenko, A. de Visser, preprint cond-mat/0109043.